STRUCTURAL CONTROL BY THE USE OF PIEZOELECTRIC ACTIVE MEMBERS

J. L. Fanson and

J.-C. Chen

Jet Propulsion Laboratory

Applied Technologies Section

California Institute of Technology

Pasadena, California

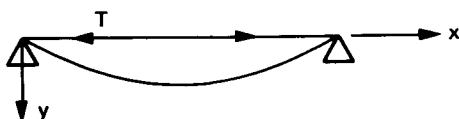# LARGE SPACE STRUCTURE CONTROL PROBLEM

Large Space Structures (LSS) exhibit characteristics which make the LSS control problem different from other control problems. LSS will most likely exhibit low-frequency, densely spaced and lightly damped modes. In theory the number of these modes is infinite. Because these structures are flexible, Vibration Suppression is an important aspect of LSS operation. There are a number of implementability issues which must be dealt with by any "space realizable" actuation and sensing scheme. In terms of Vibration Suppression, we would like the control actuators to be as low mass as possible, have infinite bandwidth, and be electrically powered. In addition, we argue that actuators which produce "internal forces" in the structure have distinct advantages for the Vibration Suppression application. Since velocity sensing may be very difficult at low vibration levels and low frequencies, we prefer to use strain as the only measurement. Finally, we propose that actuators be built into the structure as dual-purpose structural elements in the interest of efficiency of design.

- **LOW FREQUENCY, DENSELY SPACED AND LIGHTLY DAMPED MODES ARE COMMON. ACCURATE SYSTEM CHARACTERISTICS ARE DIFFICULT TO OBTAIN**

- **VIBRATION SUPPRESSION IS AN IMPORTANT ASPECT OF LSS OPERATION**

- **ACTUATOR REQUIREMENTS ARE LIGHT WEIGHT, INTERNAL FORCE PRODUCING, ELECTRICAL POWERED, INFINITE BANDWIDTH, etc.**

- **ACCURATE VELOCITY SENSING MAY BE UNREALISTIC**

- **STRAIN SENSORS SHOULD BE CONSIDERED**

- **INTEGRATED DUAL PURPOSE LOAD CARRYING/ACTUATION MEMBERS SHOULD BE CONSIDERED**
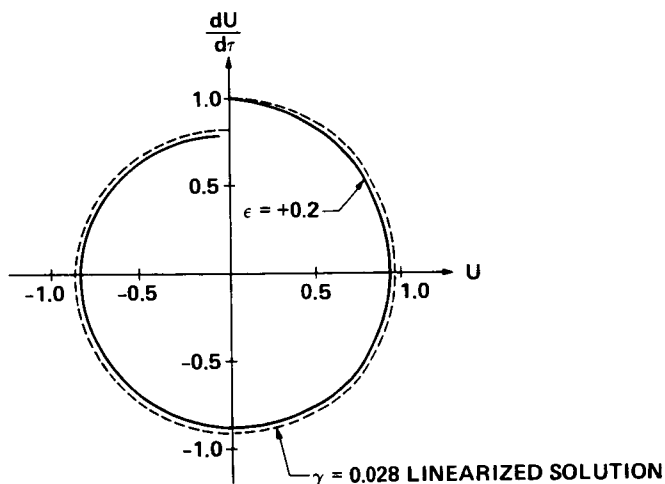
STIFFNESS CONTROL

Initial work investigating vibration suppression in LSS using internal forces centered on the one-dimensional vibrating string. The string has low inherent out-of-plane stiffness, like some Large Space Structures. It was found that by varying the tension in the string as a function of state variables and time, damping could be introduced. The lower figure shows a plot of the motion of the string in the phase plane. The distance of the curve from the origin is an indication of the energy in the motion at a particular point in time. The damping is evident by the spiraling of the locus into the origin.

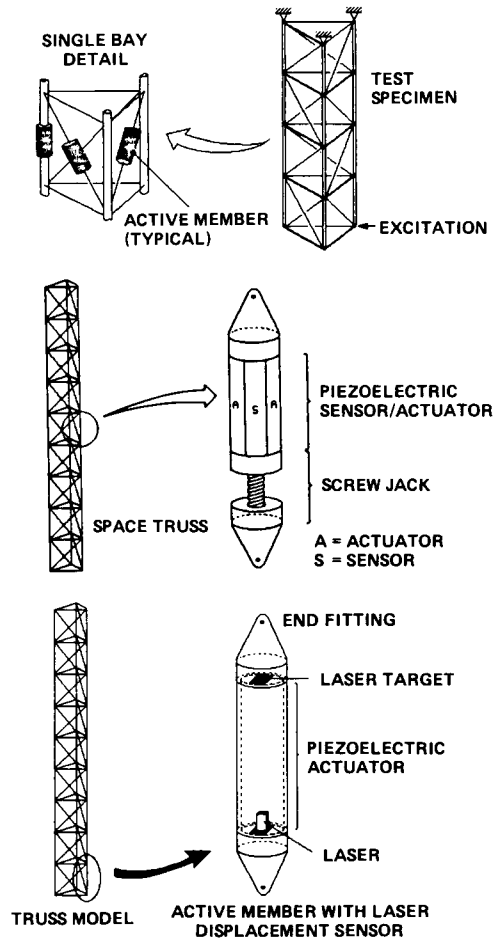**VIBRATING STRING**

$$\rho \frac{\partial^2 y}{\partial t^2} = \frac{\partial}{\partial x}\left(T \frac{\partial y}{\partial x}\right)$$

$$T = T\left(y, \frac{\partial y}{\partial t}, t\right)$$

$\epsilon = +0.2$

$\gamma = 0.028$ LINEARIZED SOLUTION

EXAMPLES OF ACTIVE MEMBERS

The concept of an active member is to replace a passive structural element, such as a diagonal of a space-truss beam, with a structure which is also a control actuator and sensor. We propose a piezoelectric active member for the control of LSS. Such devices would consist of a piezoelectric actuator and sensor for measuring strain, and screwjack actuator in series for use in quasi-static shape control. Several concepts for active-members are shown. One variation is to beam a laser through a hollow strut to measure movement between the two ends of the member. We envision these devices as being self-contained, possibly containing their own electronics for effecting Vibration Suppression.

SINGLE BAY DETAIL

TEST SPECIMEN

ACTIVE MEMBER (TYPICAL)

EXCITATION

PIEZOELECTRIC SENSOR/ACTUATOR

SCREW JACK

SPACE TRUSS

A = ACTUATOR
S = SENSOR

END FITTING

LASER TARGET

PIEZOELECTRIC ACTUATOR

LASER

TRUSS MODEL

ACTIVE MEMBER WITH LASER DISPLACEMENT SENSOR

FEASIBILITY STUDY --- PIEZOBEAM EXPERIMENT

In order to investigate the feasibility of using piezoelectric active members to perform Vibration Suppression in LSS, a simple experiment was designed. The objective of the experiments is to simulate an active member using piezoelectric ceramic thin sheet material on a thin, uniform cantilever beam. The structure was designed to have low stiffness, low mass density, and to have a first mode at 5 Hz. We use collocated piezoelectric ceramics as both actuators and strain sensors. The layup of the ceramics and the dimensions of the composite piezobeam are shown.
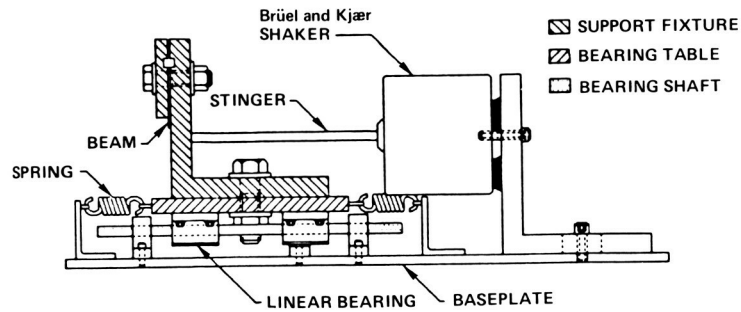
- OBJECTIVE - SIMPLE DEMONSTRATION OF VIBRATION SUPPRESSION
- INTEGRATED STRUCTURAL MEMBER/ACTUATOR
- LSS CHARACTERISTICS
  - LOW STIFFNESS
  - LOW MASS
  - HIGH MODAL DENSITY AT HIGHER FREQUENCY
- COLLOCATED ACTUATORS/SENSORS
- SPACE REALIZABLE APPROACH
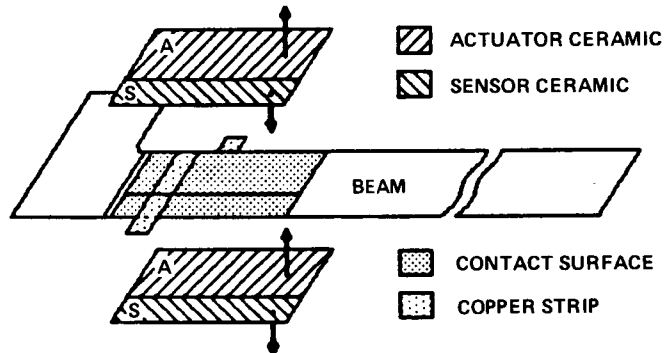
	BEAM	PIEZOELECTRIC CERAMICS	
		ACTUATOR	SENSORS
LENGTH:	12.50 in	1.25 in	1.25 in
WIDTH:	0.648 in	0.50 in	0.25 in
THICKNESS:	0.020 in	0.0095 in	0.0095 in
MATERIAL:	ALUMINUM	LEAD-ZIRCONATE-TITANATE (PZT)	

The cantilever beam was supported in a vibration test fixture shown in the figure. The beam was supported in a clamping flange which was bolted to a linear bearing table. The table was excited by means of a stinger attached to a small shaker. A wide variety of waveforms were used to test the open-loop and closed-loop performance of the piezobeam.
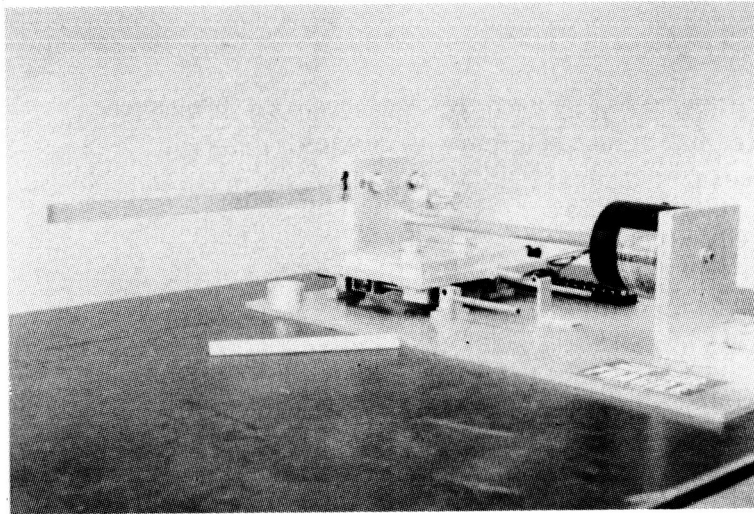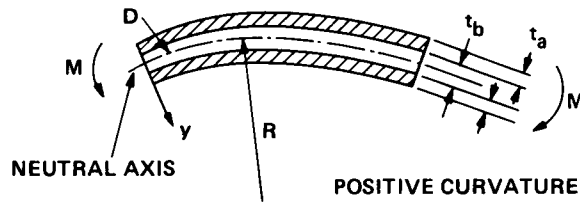
MECHANICS OF PIEZOELECTRICS

The piezoelectric ceramic material is an inherent electromechanical transducer. If an electric field is applied to the material, it tends to strain by an amount proportional to the strength of the applied field. The proportionality constant is the d_{31} coefficient. If, on the other hand, the material is stressed, an electric field is generated spontaneously. The proportionality constant between stress and generated electric field is the g_{31} coefficient. Both the d_{31} and the g_{31} coefficients are material properties of the piezoelectric.

The piezoelectrics are arranged on the test beam in a sandwich fashion. The actuators are arranged such that a voltage applied to the outer electrode surfaces causes one ceramic to expand while the other contracts. Since the ceramics are adhered to the beam, a bending moment is produced. Similarly, the bending of the beam stresses the sensor ceramics which in turn produce a voltage which is measured.

(a.) ACTUATOR PIEZOELECTRIC

E_f POLARITY

CERAMIC

$\leftarrow$ 1.0 $\rightarrow$ | $\leftarrow$ ϵ_E

$\epsilon_E = d_{31} E_f,$

(b.) SENSOR PIEZOELECTRIC

E_f POLARITY

$\sigma \rightarrow$ $\leftarrow \sigma$

$E_f = -g_{31} \sigma,$

V_a = ACTUATOR VOLTAGE

d_{31} = PIEZOELECTRIC STRAIN CONSTANT

g_{31} = PIEZOELECTRIC VOLTAGE CONSTANT

t_a = THICKNESS OF THE ACTUATOR CERAMICS

PUSH-PULL BENDING ACTUATOR

POLARITY $\bullet V_a$

CERAMIC

ALUMINUM

CERAMIC

POLARITY $\bullet V_a$

The moment applied by the piezoelectrics is determined by integrating the stress produced. The magnitude of the applied moment is found to be proportional to the width of the actuator ceramic W_a, the product of the Young's Modulus and piezoelectric strain constant $d_{31} E_a$, the "lever arm" (or distance from the neutral axis), and the applied voltage V_a. The measured voltage was about 25% less than the predicted value which is consistent with the simplifying assumptions of the analysis.

ACTUATOR INDUCED BENDING MOMENT

NEUTRAL AXIS

POSITIVE CURVATURE

$$M = \int_A \sigma_x (y - D)\, dA = \int_A E\, \epsilon_x (y - D)\, dA.$$

$$= \int_{\substack{\text{UPPER} \\ \text{CERAMICS}}} E_1\, (-\epsilon_E)\, (y - D)\, dA + \int_{\substack{\text{LOWER} \\ \text{CERAMICS}}} E_3\, (\epsilon_E)\, (y - D)\, dA.$$

$$M = W_a E_a d_{31} (t_a + t_b)\, V_a.$$

$$M = 1.02 \times 10^{-3}\, V_a\, \frac{\text{in} \cdot \text{lb}_f}{\text{VOLT}}$$

ACTUAL MEASUREMENT: $M = 0.714 \times 10^{-3}\, V_a\, \dfrac{\text{in} \cdot \text{lb}_f}{\text{VOLT}}$

The sensor responds to the applied stress. Assuming that the stress at the midthickness is the sensor stress σ_s, we find that the sensor responds to the curvature of the beam $\frac{\partial^2 y}{\partial x^2}$. Again, using the modal expansion, we find that the sensor voltage is a function of the curvature of the mass-normalized mode shape. This measurement is related to the bending strain of the beam which is a generalized displacement.

SENSOR: PLANT TRANSFER FUNCTION

THE SENSOR SENSES THE MODAL "DISPLACEMENT"

$$\sigma_s = -\frac{1}{2}(t_s + t_b)\frac{M}{I}.$$

$$V_s = -\frac{1}{2}g_{31} t_s (t_s + t_b)\frac{M}{I}.$$

$$V_s \doteq \underbrace{\frac{1}{2}f_s g_{31} t_s (t_s + t_b) E_b}_{a_2} \frac{\partial^2 y}{\partial x^2},$$

f_s = SENSOR CALIBRATION FACTOR = 0.75

$$V_s = a_2 C \left(\frac{\partial^2 y}{\partial x^2}\right),$$

C = FACTOR FOR CURVATURE VARIATION

$$V_s = a_2 \xi_i(t) C \left(\frac{\partial^2 \phi_i(x)}{\partial x^2}\right) = a_2 \xi_i(t) C_i.$$

*THE SENSOR SENSES THE MODAL "DISPLACEMENT".

EQUATION OF MOTION FOR PIEZOBEAM

    The partial differential equation of motion for the piezobeam is shown. It involves the second spatial derivative of the applied moment. The actuators are modelled as applying a uniform distributed follower moment over part of the length of the beam. The applied moment is modelled mathematically using a Heaviside Step function to turn the moment on and another Heaviside Step to turn it off spatially. Using the standard modal expansion, the modal equations are derived. The coupling of the actuator to the modal equations involves the difference in slopes of the mass-normalized mode shapes at the ends of the actuator ceramics.
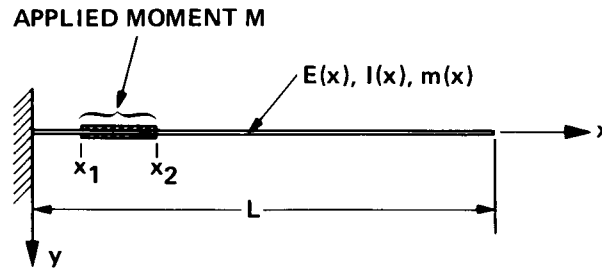
$$m(x)\frac{\partial^2 y}{\partial t^2} + \frac{\partial^2}{\partial x^2}\left(E(x)\,I(x)\,\frac{\partial^2 y}{\partial x^2}\right) = \frac{\partial^2 M(x)}{\partial x^2}\ .$$

$$M(x) = a_1 V_a\,[h(x-x_1) - h(x-x_2)],$$

$$h(\cdot) = \text{HEAVISIDE STEP FUNCTION}$$
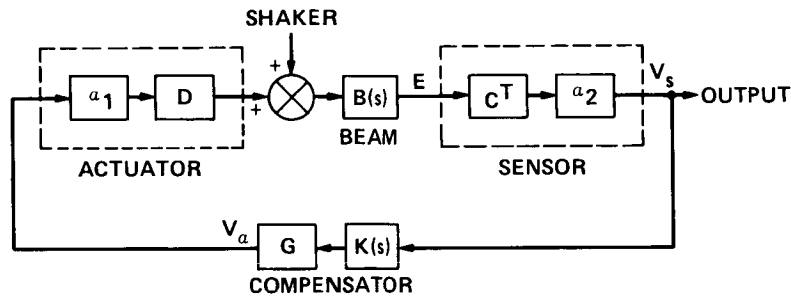
MODAL EQUATIONS:

$$y(x,t) = \sum_{i=1}^{n} \xi_i(t)\,\phi_i(x).$$

$$\ddot{\xi}_j(t) + \xi_j(t)\,\omega_j^2 = a_1 D_j V_a.$$

WHERE $\quad D_j \equiv [\phi_j'(x_2) - \phi_j'(x_1)],$

SYSTEM CONFIGURATION

The top figure is a block diagram of the control system. The actuators and sensors are modelled as non-dynamic real constant matrices. The external disturbances enter through the shaker. The control approach used in these experiments is called Positive Position Feedback. This technique uses displacement measurements to effect vibration suppression. It can be understood by considering the scalar case consisting of two equations, one representing the structure or mode ζ, and one representing a tuned control filter η. The modal displacement drives the filter, and the filter coordinate is fed back in turn to the structure. The Positive Position terminology can be understood from these equations.

SHAKER

```
               + ↓
 ┌────────────┐   ⊗   ┌──────┐  E  ┌──────────┐       V_s
 │ a₁   D     │ + →│B(s)│────→│ cᵀ   a₂ │────→ →OUTPUT
 └────────────┘       └──────┘     └──────────┘
   ACTUATOR           BEAM            SENSOR

         V_a ┌───┐   ┌────┐
       ──────│ G │←──│K(s)│←────────
             └───┘   └────┘
            COMPENSATOR
```

SYSTEM EQUATIONS FOR SISO:

STRUCTURE: $\ddot{\xi} + 2\zeta\omega\dot{\xi} + \omega^2\xi = g\omega^2\eta + f(t)$

COMPENSATOR: $\ddot{\eta} + 2\zeta_f\omega_f\dot{\eta} + \omega_f^2\eta = \omega_f^2\xi$

ω = MODAL FREQUENCY , ζ = MODAL DAMPING

g = GAIN FACTOR   , f = EXTERNAL FORCE

ω_f = FILTER FREQUENCY , ζ_f = FILTER DAMPING
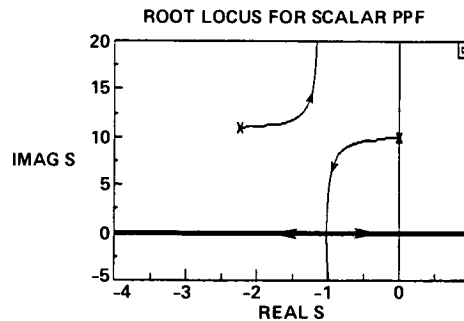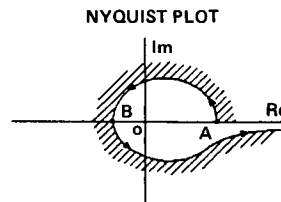
POSITIVE POSITION FEEDBACK (PPF) CONTROL

- POSITION COORDINATE OF THE STRUCTURE IS POSITIVELY FED TO THE FILTER

- POSITION COORDINATE OF THE FILTER IS POSITIVELY FED BACK TO THE STRUCTURE

The system matrix equation for the scalar example shows that the coupling of the structure to the compensator occurs in the frequency or stiffness matrix. This is because displacements are used as measurement quantities. A stability analysis of the system equation indicates that stability is maintained if the gain g lies between zero and one. In particular, the point on the Nyquist plot which determines stability is the point A. If point A lies to the right of the origin, stability is maintained. Point A is the point on the locus corresponding to zero frequency. Thus the stability criterion is non-dynamic. This is characteristic of Positive Position Feedback and accounts for the improved robust stability of this method. A root locus for the scalar case shows how PPF achieves Vibration Suppression. The filter pole moves toward the imaginary axis while the structural pole moves into the left half plane. Thus, the structural pole is stabilized.

$$\begin{Bmatrix} \ddot{\xi} \\ \ddot{\eta} \end{Bmatrix} + \begin{bmatrix} 2\zeta\omega & 0 \\ 0 & 2\zeta_f\omega_f \end{bmatrix} \begin{Bmatrix} \dot{\xi} \\ \dot{\eta} \end{Bmatrix} + \begin{bmatrix} \omega^2 & -g\omega^2 \\ -\omega_f^2 & \omega_f^2 \end{bmatrix} \begin{Bmatrix} \xi \\ \eta \end{Bmatrix} = 0$$

THE CONTROL GAIN FACTOR IS IN THE SYSTEM STIFFNESS
MATRIX, THUS THE TERM "STIFFNESS CONTROL".

NYQUIST PLOT

ROOT LOCUS FOR SCALAR PPF

POSITIVE POSITION FILTER DESIGN

The Positive Position Feedback compensator is composed of tuned filters with transfer function shown below. A simple analog filter realization with the desired transfer function is shown. The frequency and damping ratio is selected based on the results of the control synthesis.

LAPLACE TRANSFORM OF FILTER

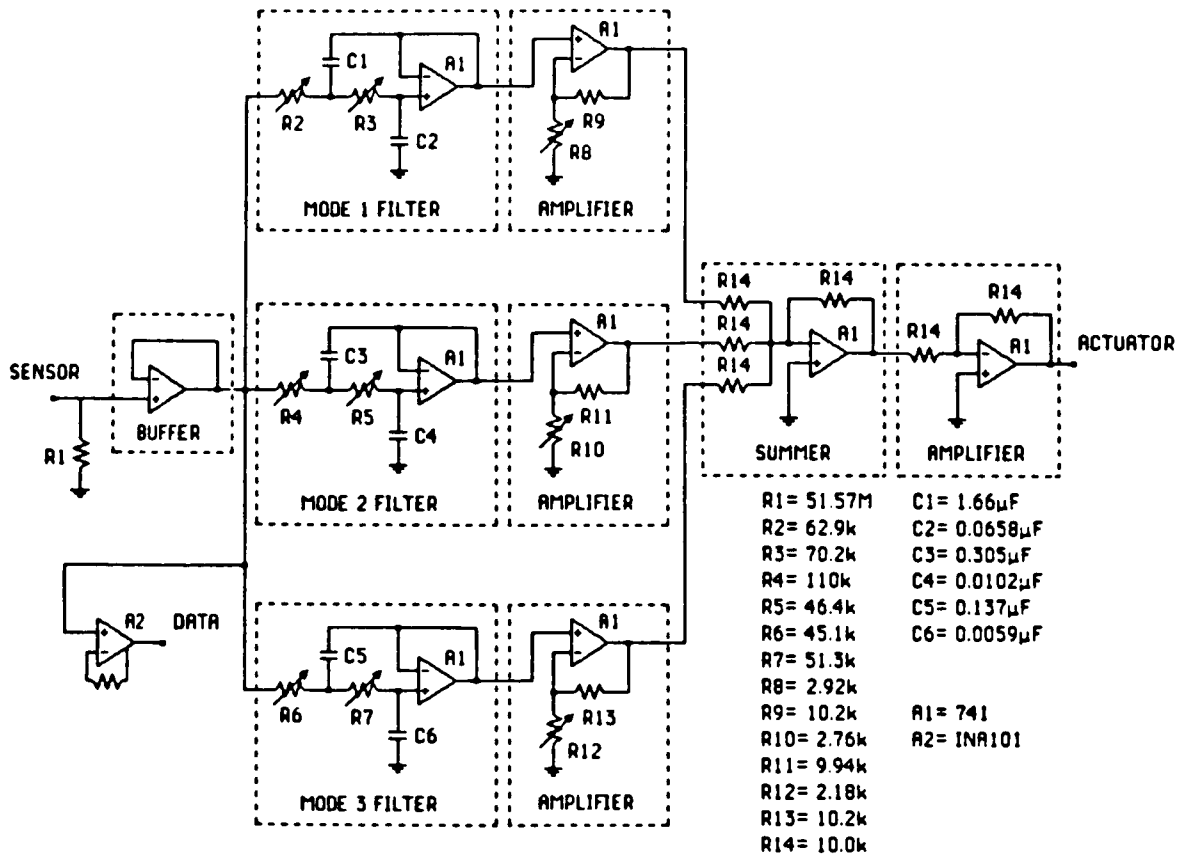$$T(s) = \frac{\omega_f^2}{s^2 + 2\zeta f \omega fs + \omega_f^2},$$
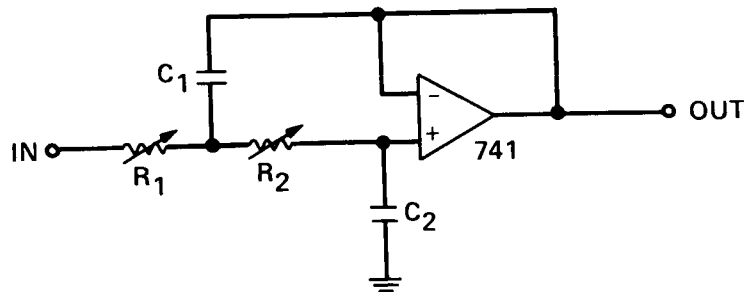
$$\omega_f = \sqrt{\frac{1}{R_1 R_2 C_1 C_2}},$$

$$\zeta_f = \frac{1}{2}\omega_f (R_1 + R_2) C_2.$$
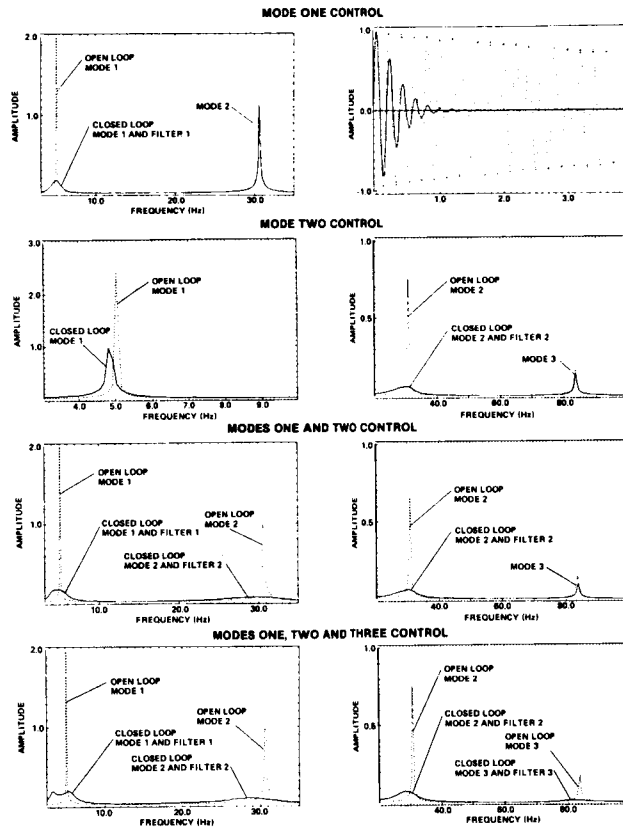
$$R_1 = R_2 \cong 50 \, K \, (OHMS)$$

Several experiments were performed. The first experiments controlled the lower modes of the beam individually with one sensor and actuator pair. Then the lower modes were controlled together. The control circuit for the control of the first three modes is shown along with the component values used. The circuit contains more amplifiers than necessary to allow more flexibility in the development of the experiment.

R1= 51.57M C1= 1.66μF
R2= 62.9k   C2= 0.0658μF
R3= 70.2k   C3= 0.305μF
R4= 110k   C4= 0.0102μF
R5= 46.4k   C5= 0.137μF
R6= 45.1k   C6= 0.0059μF
R7= 51.3k
R8= 2.92k
R9= 10.2k   A1= 741
R10= 2.76k A2= INA101
R11= 9.94k
R12= 2.18k
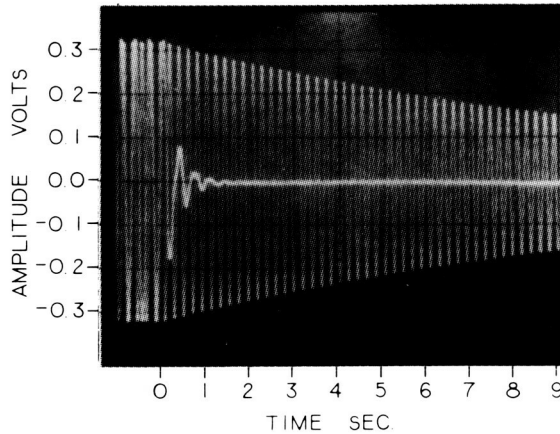R13= 10.2k
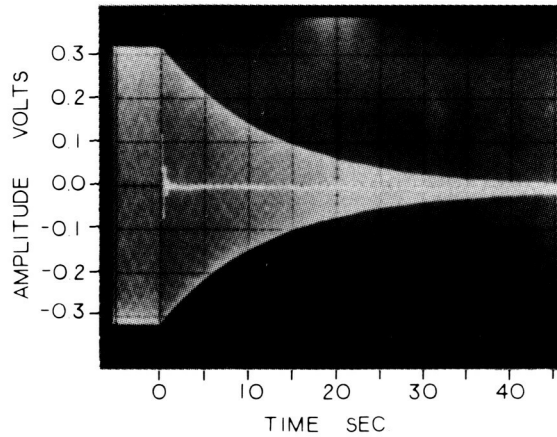R14= 10.0k

SISO EXPERIMENTAL RESULTS

The frequency response functions for the experiments using one actuator and sensor pair are shown. These are measured data. The dashed line represents the open-loop response, the solid line represents the closed-loop response. It can be seen that the control action on the controlled modes greatly reduces their response amplitude. In addition, the spillover into uncontrolled modes is always stabilizing. This is characteristic of Positive Position Feedback. The open-loop and closed-loop free decay for Mode 1 under Mode 1 control is also shown.

Oscilloscope photographs of the free decay of Mode 1 under three mode control are shown. Each photograph shows the open-loop decay as the outer envelope, and the closed-loop decay as the inner trace. Both photographs are of the same response only at two different time scales. The settling time of the first mode was reduce from about one minute to about one second.

OPEN AND CLOSED LOOP FREE DECAY OF MODE ONE
FOR THREE MODE CONTROL

824

These tables summarize the open-loop and closed-loop performance for the single-input-single-output experiments. Three quantities of interest are compared: ζ, $\zeta\omega_n$, and $\zeta\omega_n^2$. The first quantity, ζ, is the damping ratio and is a general measure of modal damping. The second quantity, $\zeta\omega_n$, is inversely related to the settling time. The third quantity, $\zeta\omega_n^2$, is inversely related to the steady-state amplitude of response to sinusoidal excitation ignoring the effects of mode shape changes. Depending on the type of dynamic response of interest one or another of these quantities is of greater interest.

EFFECT OF MODE 1 CONTROL ON MODES 1 AND 2

	MODE 1			MODE 2		
	$\zeta_1(\%)$	$\zeta_1\omega_1$	$\zeta_1\omega_1^2$	$\zeta_2(\%)$	$\zeta_2\omega_2$	$\zeta_2\omega_2^2$
OPEN LOOP	0.23	0.0721	2.27	0.15	0.289	55.5
CLOSED LOOP	16.3	4.68	135.	0.19	0.366	70.3
PERCENT CHANGE*	7,000	6,400	5,800	26.7	26.6	26.7
PREDICTED†	13.3	3.96	118.	0.17	0.320	61.7

EFFECT OF MODE 2 CONTROL ON MODES 1 AND 2

	MODE 1			MODE 2		
	$\zeta_1(\%)$	$\zeta_1\omega_1$	$\zeta_1\omega_1^2$	$\zeta_2(\%)$	$\zeta_2\omega_2$	$\zeta_2\omega_2^2$
OPEN LOOP	0.23	0.0721	2.27	0.15	0.289	55.5
CLOSED LOOP	0.43	0.131	4.00	12.7	22.4	3.95×10^3
PERCENT CHANGE*	87	80	76	8,400	7,700	7,000
PREDICTED†	0.37	0.112	3.40	13.3	23.5	4.18×10^3

EFFECT OF TWO MODE CONTROL ON MODES 1 AND 2

	MODE 1			MODE 2		
	$\zeta_1(\%)$	$\zeta_1\omega_1$	$\zeta_1\omega_1^2$	$\zeta_2(\%)$	$\zeta_2\omega_2$	$\zeta_2\omega_2^2$
OPEN LOOP	0.23	0.0721	2.27	0.15	0.289	55.5
CLOSED LOOP	15.3	3.81	94.7	13.8	23.7	4.05×10^3
PERCENT CHANGE*	6,600	5,200	4,100	9,100	8,100	7,200
PREDICTED†	12.7	3.38	89.9	12.7	22.8	4.07×10^3

EFFECT OF THREE MODE CONTROL ON MODES 1, 2, AND 3

|	MODE 1			MODE 2			MODE 3		
	$\zeta_1(\%)$	$\zeta_1\omega_1$	$\zeta_1\omega_1^2$	$\zeta_2(\%)$	$\zeta_2\omega_2$	$\zeta_2\omega_2^2$	$\zeta_3(\%)$	$\zeta_3\omega_3$	$\zeta_3\omega_3^2$
OPEN LOOP	0.23	0.0721	2.27	0.15	0.289	55.5	0.27	1.41	738.
CLOSED LOOP	13.4	2.63	51.5	8.85	15.7	2.78×10^3	3.99	20.4	1.04×10^4
PERCENT CHANGE*	5,700	3,500	2,200	5,800	5,300	4,900	1,400	1,300	1,300
PREDICTED†	–	–	–	–	–	–	–	–	–

* PERCENT CHANGE BETWEEN MEASURED VALUES

† PREDICTED CLOSED LOOP VALUES

Two sensors and actuators were used in a multi-input-multi-output experiment to control the first six modes of the beam. The location of the two sets is shown in the figure. The open-loop and closed-loop frequency response functions are shown for the first eight modes.

ACTUATOR/SENSOR LOCATIONS FOR MIMO PIEZOBEAM.
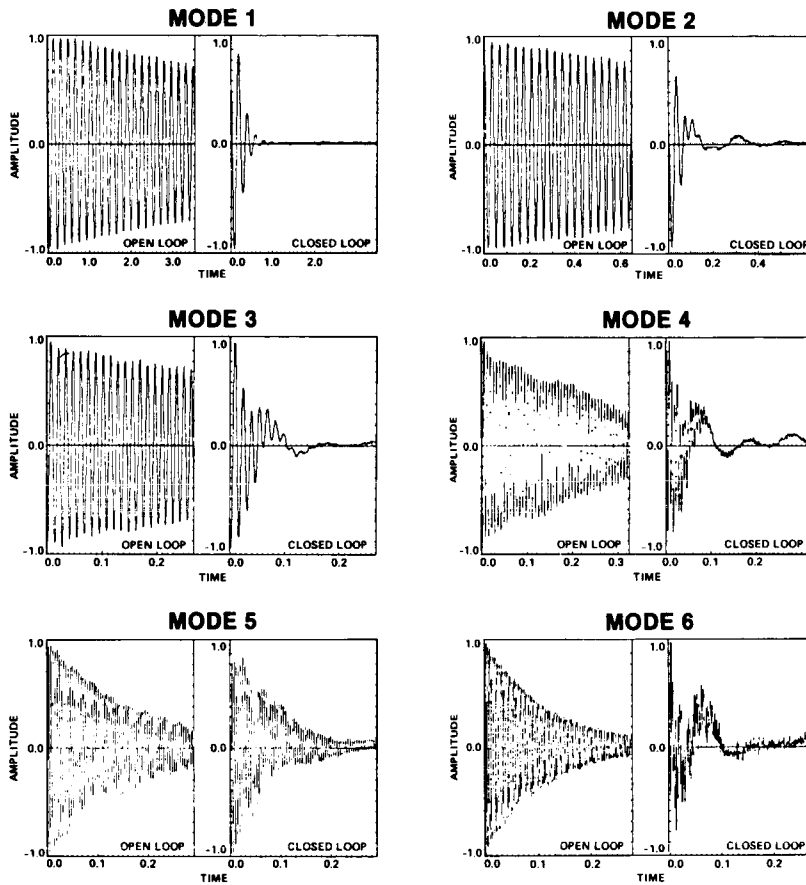## ALL DIMENSIONS IN INCHES.
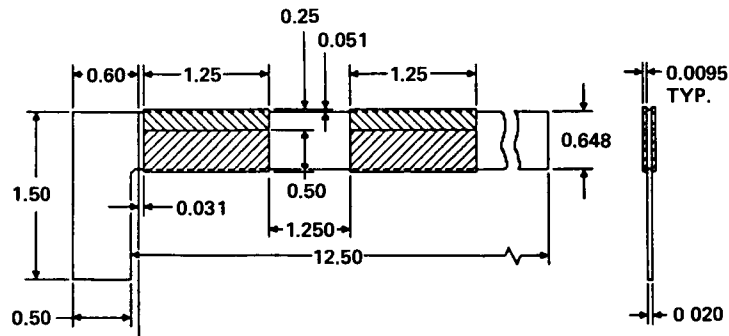
OPEN LOOP AND MIMO CLOSED LOOP FREQUENCY
RESPONSE FUNCTIONS FOR SENSOR 1.
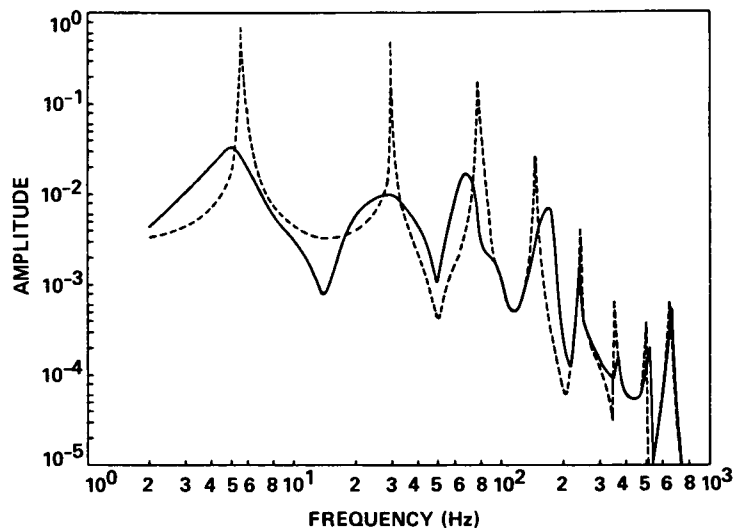
The open-loop and closed-loop free decay responses for the first six modes of the beam are shown.

OPEN LOOP AND CLOSED LOOP FREE DECAY

The two tables summarize the open-loop and closed-loop performance for the six mode control case.

EFFECT OF MIMO CONTROL ON MODES 1 THROUGH 8

	MODE 1			MODE 2			MODE 3			MODE 4		
	$\zeta_1(\%)$	$\zeta_1\omega_1$	$\zeta_1\omega_1^2$	$\zeta_2(\%)$	$\zeta_2\omega_2$	$\zeta_2\omega_2^2$	$\zeta_3(\%)$	$\zeta_3\omega_3$	$\zeta_3\omega_3^2$	$\zeta_4(\%)$	$\zeta_4\omega_4$	$\zeta_4\omega_4^2$
OPEN LOOP	0.33	0.116	4.11	0.19	0.352	64.1	0.23	1.05	489.	0.38	3.54	3.30×10^3
CLOSED LOOP	20.0	5.93	176.	24.8	34.0	4.65×10^3	8.00	33.2	1.38×10^4	4.05	29.8	2.19×10^4
PERCENT CHANGE[*]	*6,000*	*5,000*	*4,200*	*13,000*	*9,600*	*7,200*	*3,400*	*3,100*	*2,700*	*970*	*740*	*560*
PREDICTED[†]	31.5	8.47	200.	18.6	28.8	4.44×10^3	13.4	52.5	2.06×10^4	5.44	41.0	3.08×10^4

	MODE 5			MODE 6			MODE 7			MODE 8		
	$\zeta_5(\%)$	$\zeta_5\omega_5$	$\zeta_5\omega_5^2$	$\zeta_6(\%)$	$\zeta_6\omega_6$	$\zeta_6\omega_6^2$	$\zeta_7(\%)$	$\zeta_7\omega_7$	$\zeta_7\omega_7^2$	$\zeta_8(\%)$	$\zeta_8\omega_8$	$\zeta_8\omega_8^2$
OPEN LOOP	0.39	5.73	8.42×10^3	0.37	7.98	1.73×10^4	0.34	10.6	3.32×10^4	0.36	11.3	3.55×10^4
CLOSED LOOP	0.78	11.4	1.68×10^4	0.62	14.1	3.14×10^4	0.45	15.9	5.09×10^4	0.50	16.2	5.20×10^4
PERCENT CHANGE[*]	*100*	*100*	*100*	*70*	*80*	*80*	*46*	*50*	*53*	*40*	*43*	*46*
PREDICTED[†]	3.24	46.9	6.81×10^4	3.03	64.7	1.38×10^5	–	–	–	–	–	–

[*] PERCENT CHANGE BETWEEN MEASURED VALUES   [†] PREDICTED CLOSED LOOP VALUES

CONCLUSIONS

The conclusions drawn from this analysis and these experiments follow.

- FEASIBILITY OF USING PIEZOELECTRIC MATERIALS AS DUAL-PURPOSE STRUCTURAL ELEMENTS/ACTUATORS FOR VIBRATION SUPPRESSION IN LARGE SPACE STRUCTURES WAS DEMONSTRATED

- POSITIVE POSITION FEEDBACK (PPF) AS A VIBRATION SUPPRESSION CONTROL STRATEGY WAS IMPLEMENTED

- USING THE STRAIN SENSOR WHICH MEASURES THE ELASTIC DEFORMATION FOR CONTROL WAS SUCCESSFULLY DEMONSTRATED

- MULTI-MODE VIBRATION SUPPRESSION WAS ACHIEVED WITH DRAMATIC REDUCTION IN DYNAMIC RESPONSE

- NO DESTABILIZING EFFECTS WERE OBSERVED DUE TO EITHER THE SPILLOVER OR THE ACTUATOR DYNAMICS

- A BETTER SYNTHESIS THEORY WHICH PROVIDES PROCEDURES FOR THE SELECTION OF GAINS FOR STRONG STRUCTURE/CONTROL COUPLING SHOULD BE DEVELOPED

- A TRUE ACTIVE MEMBER NEEDS TO BE DEVELOPED AND INCORPORATED INTO MORE COMPLICATED EXPERIMENTS